Photoacoustics 23 (2021) 100283

Contents lists available at ScienceDirect

Photoacoustics

journal homepage: www.elsevier.com/locate/pacs

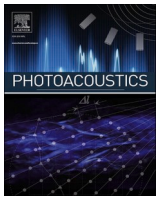

Research article

Multispectral optoacoustic tomography of lipid and hemoglobin contrast in human carotid atherosclerosis

Angelos Karlas [a,b,c,d,1], Michael Kallmayer [c,1], Michael Bariotakis [a,b], Nikolina-Alexia Fasoula [a,b], Evangelos Liapis [a,b], Fabien Hyafil [e,f], Jaroslav Pelisek [c,g], Moritz Wildgruber [h], Hans-Henning Eckstein [c,d,1], Vasilis Ntziachristos [a,b,d,1,*]

[a] Chair of Biological Imaging, Central Institute for Translational Cancer Research (TranslaTUM), Technical University of Munich, Munich, Germany
[b] Helmholtz Zentrum München, Institute of Biological and Medical Imaging, Neuherberg, Germany
[c] Clinic for Vascular and Endovascular Surgery, Technical University of Munich, Klinikum rechts der Isar, Munich, Germany
[d] DZHK (German Centre for Cardiovascular Research), Partner Site Munich Heart Alliance, Munich, Germany
[e] INSERM U1148, Laboratory for Vascular Translational Science (LVTS), DHU FIRE, University de Paris, Paris, France
[f] Department of Nuclear Medicine, Bichat University Hospital, Assistance-Publique-Hôpitaux de Paris, Paris, France
[g] Department of Vascular Surgery, University Hospital Zurich, Zurich, Switzerland
[h] Department of Radiology, University Hospital, LMU Munich, Munich, Germany

ARTICLE INFO

Keywords:
MSOT
Photoacoustic imaging
Carotid plaque
Stroke
Cardiovascular disease
Molecular imaging
Carotid artery stenosis

ABSTRACT

Several imaging techniques aim at identifying features of carotid plaque instability but come with limitations, such as the use of contrast agents, long examination times and poor portability. Multispectral optoacoustic tomography (MSOT) employs light and sound to resolve lipid and hemoglobin content, both features associated with plaque instability, in a label-free, fast and highly portable way. Herein, 5 patients with carotid atherosclerosis, 5 healthy volunteers and 2 excised plaques, were scanned with handheld MSOT. Spectral unmixing allowed visualization of lipid and hemoglobin content within three ROIs: whole arterial cross-section, plaque and arterial lumen. Calculation of the fat-blood-ratio (FBR) value within the ROIs enabled the differentiation between patients and healthy volunteers ($P = 0.001$) and between plaque and lumen in patients ($P = 0.04$). Our results introduce MSOT as a tool for molecular imaging of human carotid atherosclerosis and open new possibilities for research and clinical assessment of carotid plaques.

1. Introduction

Non-invasive carotid imaging techniques, such as ultrasound (US), magnetic resonance imaging (MRI), positron emission tomography (PET) and computed tomography angiography (CTA), aim to characterize several morphological, functional or biochemical parameters associated with plaque 'vulnerability' and, thus, help estimate the risk of ischemic stroke [1,2]. Such parameters include the grade of stenosis, arterial wall remodelling, presence of a large lipid core and a thin fibrous cap, inflammation, intraplaque hemorrhage or neovascularization and nodular calcifications [3]. Nevertheless, current radiological modalities may require: i) the intravenous administration of possibly toxic contrast agents, ii) long examination times or iii) bulky and expensive infrastructure, all characteristics not suited for highly disseminated use [4–6].

Multispectral optoacoustic tomography (MSOT) is a novel imaging technique that enables non-invasive, label-free and portable imaging of vasculature and soft tissues, such as the carotids and peripheral arteries [7,8], skeletal muscles [9–11] and adipose tissues [12–15]. In MSOT, series of light pulses with pulse widths in the 10 ns range illuminate tissues at different near-infrared wavelengths (680−980 nm), a spectral range that allows several cm of light penetration in tissue. Absorption of light by different tissue chromophores, such as hemoglobin and lipids generates ultrasound waves within tissue, which propagate to the tissue surface and are recorded at framerates of up to 50 Hz (real-time imaging) [16]. Using spectral unmixing, the recorded spectrum for each pixel

* Corresponding author at: Chair of Biological Imaging, Central Institute for Translational Cancer Research (TranslaTUM), Technical University of Munich, Munich, Germany.
E-mail address: v.ntziachristos@helmholtz-muenchen.de (V. Ntziachristos).
[1] These authors contributed equally.

https://doi.org/10.1016/j.pacs.2021.100283
Received 24 June 2020; Received in revised form 7 July 2021; Accepted 8 July 2021
Available online 9 July 2021

is decomposed into a set of known spectra of these light-absorbing molecules and reveals the distribution of each molecule within the imaged region. Modern MSOT is equipped with hand-held probes that consist of the illumination unit and the ultrasound detector and offer dual operation (MSOT/US) by also performing ultrasound imaging. In analogy to stand-alone ultrasonography, the handheld MSOT probe is placed on the skin and records high-resolution (≈ 200−300 μm) tomographic images at depths of ≈ 2−4 cm with a field of view of ≈ 4 cm [17].

Herein, we aim at investigating the MSOT capabilities as a non-invasive, label-free imaging technique for human carotid atherosclerosis, providing information relevant to intraplaque hemorrhage or neovascularization and plaque lipid content; two major determinants of plaque instability [3]. Furthermore, considering previous studies on optoacoustic imaging of atherosclerotic plaques using contrast-enhanced MSOT or optoacoustic microscopy [18,19], we further explore the capabilities of MSOT to provide *ex vivo* label-free characterization of carotid plaque tissue in selected cases.

2. Methods

We examined five ($n_1 = 5$) patients (2 F 3 M, 2 symptomatic, 3 asymptomatic, age: 65.5 ± 5.1 years) with previously diagnosed carotid atherosclerosis unilaterally in the bulb region, and five ($n_2 = 5$) healthy volunteers (2 F, 3 M, age: 33.6 ± 3.7 years) using a hybrid clinical MSOT/US system (Acuity®, iTheraMedical GmbH, Munich, Germany) described in detail elsewhere [17]. Patients and healthy volunteers signed an informed consent approved by Helmholtz Center Munich and the Technical University of Munich. Subjects were placed in supine position and scanned unilaterally over different positions along the carotid artery for almost 2 min in total. More specifically, each carotid artery was scanned with the MSOT probe placed in transverse position and moved at steps of ≈ 5 mm along the lateral aspect of the neck. Short videos (≈ 10 s) were recorded at selected positions (e.g. were the plaque was prominent for the patient group). The dominant side was selected for the healthy volunteers. By illuminating with pulses of 28 near-infrared wavelengths (700−970 nm at 10 nm-steps), we acquired multiple sets of 28 wavelengths or 'multispectral stacks' of the arterial cross-section (Fig. 1a). With a framerate of 25 Hz, each 28-wavelength multispectral stack lasted approximately 1 s. In parallel, for each MSOT frame a co-registered US frame was recorded, yet at a rate of ≈ 8 Hz, as defined by the technical specifications of our system.

Three characteristic multispectral stacks were selected for each healthy volunteer or patient to be further analysed (15 stacks for each group). During the frame selection process for the patient group, we ensured that the atherosclerotic plaque was clearly depicted in all corresponding US images. Next, the selected optoacoustic multispectral stacks were spectrally unmixed and four new images were produced: i) for oxygenated hemoglobin (HbO_2), ii) for deoxygenated hemoglobin (Hb), iii) for lipids (fat) and iv) for water (not used in the present analysis). We then calculated an image showing the spatial distribution of total hemoglobin (THb) within the imaged region, by adding the unmixed optoacoustic images of HbO_2 and Hb. Finally, we divided on a per-pixel basis the unmixed Lipids-image with the calculated THb-image to produce the final fat-blood-ratio (FBR) image for each selected multispectral stack, according to the formula FBR = fat / (fat + blood). The resulting FBR image was employed in subsequent analysis (Fig. 1b).

Manual segmentations of the artery, lumen and plaque regions of interest (ROIs) were performed in the co-registered ultrasound images with the consensus of two clinicians with wide experience in carotid artery imaging and hand-held MSOT. The efficacy of the manual segmentation step was validated by means of the Cohen's Kappa (mean ± standard error of the mean) which was 0.94 ± 0.003 for the healthy subjects and 0.92 ± 0.003 for the patients (0.93 ± 0.002 for the whole examined population). The Cohen's Kappa for each image corresponded to the mean of the pairwise Cohen's Kappa for 6 different manual segmentations performed at different time points for each selected image in consensus with two clinicians. As a last step, we extracted the mean FBR value for each manually-segmented region of interest: the whole arterial cross-section for healthy volunteers and patients, as well as the plaque and lumen area for the patient group. Further analysis of the *in vivo* MSOT data was carried out by one-tailed t- and Wilcoxon-tests.

All patients underwent elective carotid endarterectomy few days after the MSOT examination. Two excised plaques were scanned shortly after the end of the surgical operation using the same MSOT/US setup. The samples were placed in a transparent plastic pouch filled with phosphate-buffered saline and scanned for approximately 2 min along their long axis. Standard histological analysis with Hematoxylin-Eosin-(H&E), CD31- and Oil-Red-O-staining (OR) was also conducted. Consecutive segments were prepared for each plaque. One segment was fixed with formalin, embedded in paraffin (formaldehyde-fixed paraffin-embedded, FFPE), cut and stained with H&E- and CD31-staining and one segment was embedded in optimal cutting temperature (OCT) compound, cut and stained with OR-staining. The H&E-staining stained the red blood cells intensely red and revealed tissue morphology, the CD31-staining targeted the plaque neovascularization and the OR-staining stained the lipids red. Thus, the first two stainings provided information associated with the plaque blood content while the OR-staining gave insights into the lipid accumulation in the plaque (Table 1).

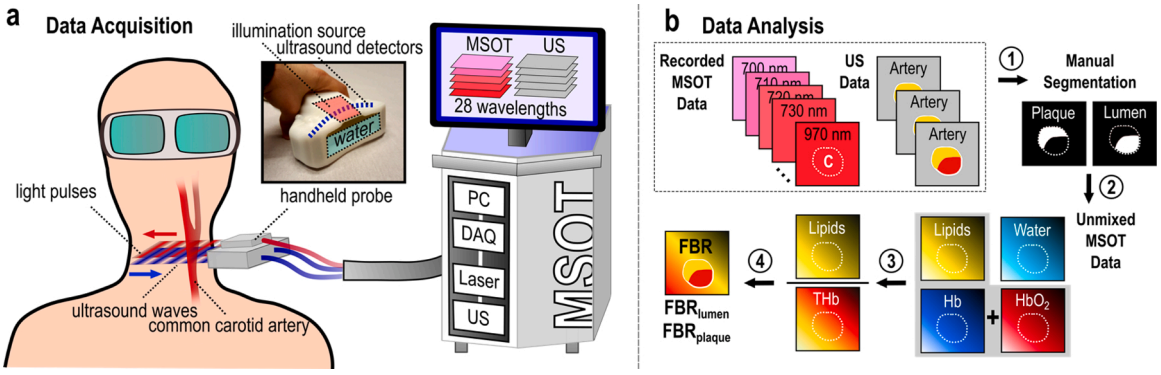

Fig. 1. MSOT principle of operation and data analysis workflow. (a) Hand-held MSOT data acquisition: Carotid artery is illuminated with pulses of multiple near-infrared light wavelengths. (b) For each light pulse/wavelength, one optoacoustic and one ultrasound frame are recorded, so that for each set of 28 wavelengths a 'multispectral stack' is generated. 1) The regions of arterial cross-section, plaque and lumen are manually segmented in the recorded ultrasound images. 2) Each multispectral stack is spectrally unmixed into four unmixed images for: HbO_2, Hb, lipids and water. 3) The HbO_2 and Hb images are added to produce a total hemoglobin (THb) image. 4) The lipids and THb are divided per pixel and a new fat-blood-ratio (FBR) image is calculated. Finally, the mean FBR value is extracted for each segmented region.

Table 1
Main histologic features of the two excised plaques scanned ex vivo.

#	Age	Sex	Class	Stability	Rupture	H&E	CD31	OR
1	60	M	AHA V	Yes	No	Collagen, Fresh Erythrocytes, Thrombus	Low	Low
2	63	W	AHA VII	No	Possible	Calcification, Necrotic Core, Thrombus	No	Medium

3. Results

Fig. 2 shows representative examples of MSOT/US images of a healthy volunteer and a patient (Fig. 2a–i). Furthermore, *ex vivo* MSOT images of the excised plaque of the same patient, and the corresponding histological analysis, are also provided (Fig. 2j–o). Fig. 2a shows a characteristic US frame taken from the lateral cervical region of a healthy volunteer. The common carotid artery is represented as a circular hypoechoic (black) region. To visualize the anatomy of the same region with MSOT (Fig. 2b), we provide the image recorded at the 800 nm, which represents the isosbestic point of HbO_2 and Hb at the near-infrared range [12,16]. The rationale behind this choice is the potent presence of hemoglobin within all tissues imaged at the lateral cervical region, which is considered to be a well-perfused anatomic area. Figs. 2c and d show the carotid artery lumen of the THb- and Lipids-images correspondingly, as calculated after spectral unmixing of the recorded MSOT data (see Methods). We observe that due to the strong presence of hemoglobin in the carotid artery lumen and the absence of plaque, the lumen is characterized by high THb- and low Lipid-signal. Fig. 2e shows the US representation of the carotid artery of a patient with carotid atherosclerosis (bulb region) and is followed by the optoacoustic visualization of the same region, recorded with MSOT at 800 nm. The arterial cross-section in the US (Fig. 2g), unmixed THb- (Fig. 2h) and unmixed Lipids-image (Fig. 2i) of the same region are also provided. Spectral unmixing reveals an intraplaque area with increased hemoglobin content (Fig. 2h), which is barely detectable in the corresponding US image (Fig. 2g). Furthermore, the unmixed Lipids-image shows high lipid absorption inside the plaque, compared to the lumen region (Fig. 2i).

The same patient underwent elective carotid endarterectomy and the excised plaque material was imaged using the same MSOT/US system, in order to investigate the capabilities of MSOT to provide label-free characterization of plaque tissue. Fig. 2j shows the US image of the excised plaque scanned along its long axis (sagittal view). Fig. 2k illustrates the co-registered unmixed optoacoustic THb-image. We observe three nodular regions of high hemoglobin content inside the plaque, which are not detectable in the corresponding US image, which provides only structural information. After the surgical extraction of the plaque, we attached a suture on the end of the plaque for orientation purposes. The suture, as highly light-absorbing material, is visible in the MSOT images, but not in the co-registered ultrasound image. Fig. 2l shows the MSOT-measured lipid signal of the excised plaque. Fig. 2m–o illustrate the histological analysis of the excised plaque sample (Table 1, plaque #1). The H&E-staining (Fig. 2m) reveals a region with rich thrombotic and fresh erythrocytes components (black dashed circle), as well as, extended collagenous structures. CD31-staining (Fig. 2n) shows a relatively poor but detectable neovascularization within the imaged plaque slice. Finally, Fig. 2o (OR-staining) shows the lipid content of the imaged plaque slice.

Fig. 3 illustrates exemplary MSOT-measured spectra within different ROIs: the whole arterial cross-section, the plaque and the lumen region (Fig. 3a). Characteristic mean measured spectra for the whole arterial cross-section (Fig. 3b) provide a clear spectral differentiation between patient and healthy arterial cross-sections. More specifically, the normalized mean spectrum of the pixels belonging to the manually segmented arterial cross-section of a healthy volunteer demonstrates an increased absorption in the wavelength range of 800−850 nm: the region where the absorption of HbO_2 is either equal (800 nm: isosbestic point of HbO_2 and Hb) or prominently higher (e.g., at 850 nm) than that of Hb [16]. Correspondingly, the mean spectrum in an arterial cross-section with a plaque shows a peak at 930 nm, where the lipids absorb the most at the NIR [12,16]. For the patient, the calculation of the mean absorption spectrum allows for differentiating between the plaque and the lumen ROI. The normalized mean lumen spectrum is

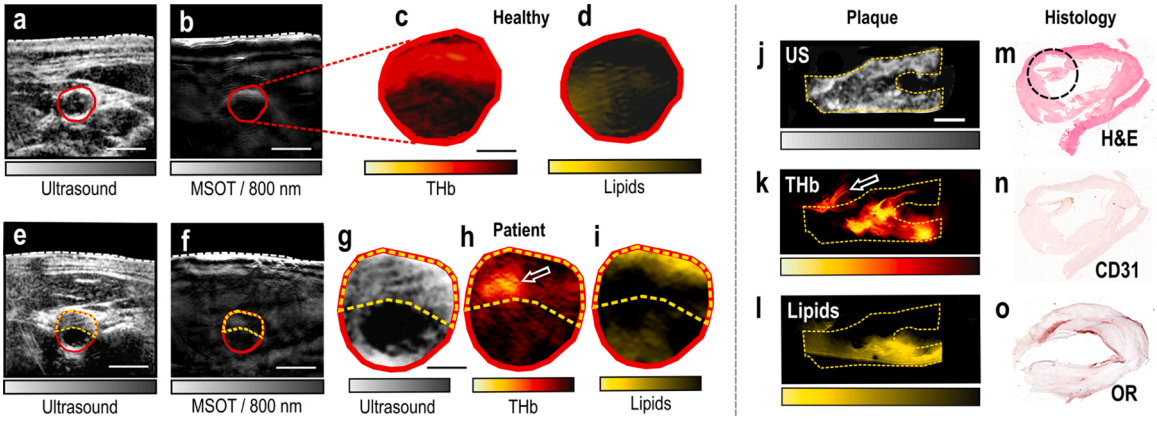

Fig. 2. MSOT/US-imaging of the carotid artery of a healthy volunteer and a patient, MSOT/US-imaging and histology of an excised plaque. (a) Recorded US image of the lateral cervical region of a healthy volunteer. (b) Corresponding MSOT image at 800 nm. White dashed line: skin surface. The carotid lumen area is demarcated in red. Scale bars: 5 mm. (c) Magnification of the lumen area of the spectrally unmixed MSOT image in (b) showing the THb-signal. (d) Same magnification showing the Lipids-signal. Scale bar: 2.5 mm. (e) Recorded US image of a patient with carotid atherosclerosis. (f) Corresponding MSOT image at 800 nm. White dashed line: skin surface. The lumen is demarcated in red and the plaque area with a yellow dashed line. Scale bars: 5 mm. (g) Magnification of the arterial cross-section in US. (h) Magnification of the arterial cross-section of the spectrally unmixed MSOT image in (f), showing the THb-signal. White arrow: region of increased THb-content. (i) Same magnification showing the Lipids-signal. Scale bar: 2.5 mm. (j) Sagittal view of the excised plaque in US. (k) Same view of the plaque in corresponding unmixed THb-image. White arrow: postoperatively attached suture. (l) Same view of the plaque in unmixed MSOT Lipids-image. Scale bar: 4 mm. (m) Histological view with H&E staining. The black circle shows a region with thrombotic and erythrocytes components. (n) Histological view with CD31-staining targeting the neovascularization. (o) Histological view with OR-staining showing the lipid content of the plaque. All presented images are exemplary. (For interpretation of the references to colour in this figure legend, the reader is referred to the web version of this article).

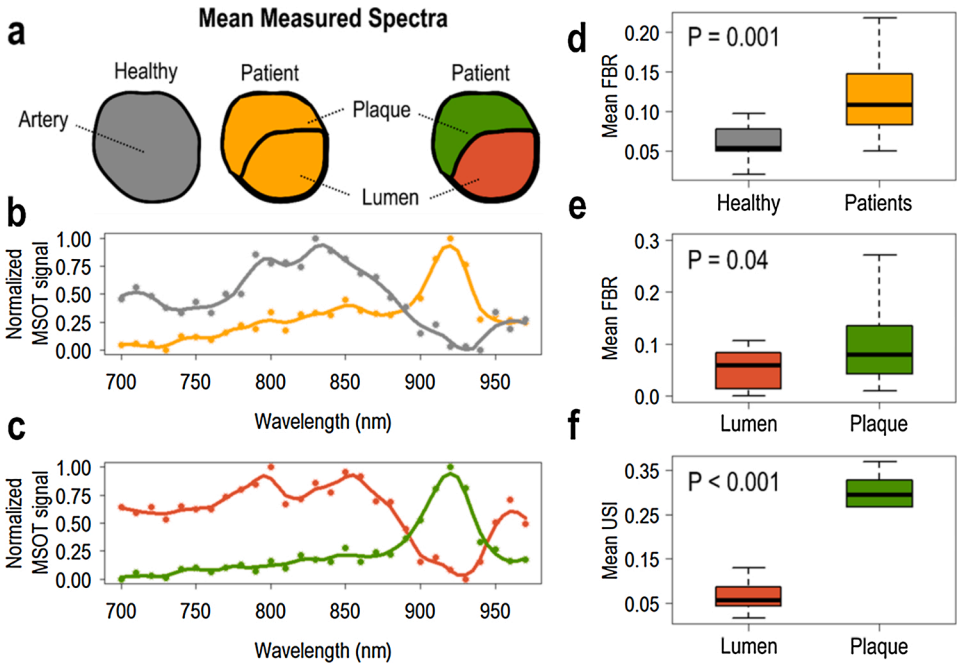

Fig. 3. Spectral, fat-blood-ratio and ultrasound intensity analysis of recorded MSOT/US data. (a) Color legend of relevant ROIs. (b) Mean spectrum of the whole arterial cross-section in a healthy volunteer (grey) and a patient (orange). (c) Mean spectrum of the lumen (red) and the plaque area (green) in a patient. (d) FBR-based differentiation between healthy volunteers and patients (whole arterial cross-section). (e) FBR-based differentiation between the lumen and the plaque region in patients. (f) USI-based differentiation between the lumen and the plaque region in patients. (For interpretation of the references to colour in this figure legend, the reader is referred to the web version of this article).

characterized by a general increase at 800−850 nm, with a peak at 850 nm, where the absorption of HbO_2 is higher compared to Hb. Moreover, the corresponding mean spectrum of the plaque pixels shows a lipid-characteristic 930 nm-peak.

Fig. 3d–f summarize the results of the FBR-based analysis (see Methods) for all relevant ROIs in the selected frames of the healthy volunteer ($3 \times n_1 = 15$) and patient ($3 \times n_2 = 15$) group. Our results show that the levels of FBR differ significantly between patients (PA) and healthy volunteers (HV) within the whole arterial cross-section (Fig. 3d; $FBR_{PA} = 0.123 \pm 0.016 > FBR_{HV} = 0.063 \pm 0.008$, $P = 0.001$). We also observe significant differences in the FBR values between the lumen (LU) and the plaque regions (PL) across the patient group (Fig. 3e; $FBR_{PL} = 0.113 \pm 0.028 > FBR_{LU} = 0.053 \pm 0.009$ for patients, $P = 0.04$). Furthermore, based on the US intensities (USI) of the images used for manual segmentation of ROIs, we successfully differentiate between the plaque and the lumen regions (Fig. 3f; $USI_{LU} = 0.068 \pm 0.01 < USI_{PL} = 0.282 \pm 0.018$, $P < 0.001$).

4. Discussion

In this preliminary study we used a hybrid hand-held MSOT/US system as a novel imaging tool for the evaluation of carotid atherosclerosis. Worldwide, almost 816 million people suffer from carotid atherosclerosis and in 58 million people the plaque causes carotid stenosis [20]. The clinical assessment of the carotid atherosclerosis is based mainly on the grade of stenosis and the presence of clinical symptoms. Current imaging techniques, such as US, CTA and MRI, attempt to provide thorough plaque assessment to detect the 'rupture-prone' plaque, which may cause ischemic stroke. However, abovementioned techniques come with limitations which hinder their disseminated use [4–6].

MSOT is a molecular imaging technique, which does not necessitate the use of intravenous contrast agents, is characterized by short examination times and is performed by portable devices, i.e., features that render MSOT appropriate for wide clinical use [16]. Herein, by conducting clinical measurements, we demonstrate the capability of MSOT to differentiate between healthy volunteers and patients, as well as, between the plaque and adjacent carotid lumen based purely on lipid and hemoglobin gradients. Thus, hand-held MSOT could serve as a label-free imaging technique for: i) detecting the presence of carotid plaque, based on direct molecular lipid and hemoglobin contrast and ii) employing this molecular contrast for *in vivo* and *ex vivo* plaque tissue characterization.

First, we show that the spectral analysis of the whole arterial cross-section enables the differentiation between healthy volunteers and patients with carotid atherosclerosis. This differentiation is purely based on endogenous lipid and hemoglobin contrast and not on indirect structural information, as provided for example by traditional US. Second, we demonstrate that MSOT is able to reveal highly-detailed (resolution of ≈ 200−300 μm) molecular information inside the plaque region, which is not detectable by US imaging. More specifically, the MSOT-extracted molecular information on lipids and hemoglobin is associated with clinically relevant factors of plaque instability, such as the intraplaque hemorrhage, the neovascularization and the lipid core. This unique capability of MSOT technology applies not only for *in vivo* but also for *ex vivo* label-free plaque imaging. Thus, MSOT may complement traditional histology by resolving endogenous chromophores within the whole volume of the excised tissue. This would possibly guide the acquisition of histology slices only at information-rich positions in order to decrease the time and the consumables needed for thorough tissue analysis.

Despite its advantages, MSOT has also limitations. Due to light attenuation with increasing depth (via scattering and absorption), the achieved penetration depth is ≈ 2−4 cm, which is low compared to currently used modalities for carotid imaging (US, CTA, MRI). Furthermore, the precise spectral unmixing remains a challenging problem, due to complex light-tissue interaction phenomena (spectral coloring effect) and motion contamination [16]. Further technical developments in the fields of laser illumination, light attenuation compensation and motion correction may overcome abovementioned limitations in the near future.

In the current study we developed and suggested the use of FBR as a biomarker to distinguish between normal and atherosclerotic arteries, as well as between the plaque and lumen regions in atherosclerotic arterial segments. Of course, a plaque is a complex tissue consisting of lipids, blood inclusions, calcifications, necrotic components, etc. in varying levels and the plaques scanned herein are no exception. Nevertheless, even if, for example, severe plaque calcifications —a feature not observed within the scanned and analysed arterial segments —were to bias the FBR assessment, we believe that the proposed FBR biomarker

would still enable the attempted differentiations (normal vs. atherosclerotic artery and arterial lumen vs. plaque) in the majority of plaques, since the lipid content of a diseased artery or plaque are expected to be higher than those of a normal artery or the arterial lumen. As a direct correlation between MSOT findings and histology analysis lies beyond the scope of this work, further studies are needed to define the efficacy of our method beyond the simple plaque detection and towards discriminating among different types of plaques with different consistencies and complexity [21].

Of course, the FBR calculation depends on the precise segmentation of the corresponding ROIs, as well as the accuracy of the spectral unmixing step. On one hand, the manual segmentation by trained experts may be validated by means of relevant metrics (e.g., Cohen's Kappa), as done in this study (*see Methods*). Also, the development of sophisticated algorithms for the automatic segmentation of the relevant vascular ROIs would also ensure an accurate FBR calculation [22]. On the other hand, the spectral unmixing strategy applied in the current study has been used in several clinical applications with good results. [11,16]. Nevertheless, the development of advanced spectral unmixing techniques for clinical MSOT applications would aid more quantitative analysis approaches.

Thus, the present preliminary study shows the unique potential of MSOT for non-invasive label-free characterization of human carotid atherosclerosis. Even if our study involves only a small number of patients and is, thus, only a first step towards a larger cohort analysis, MSOT was able to differentiate between patients and healthy volunteers, as well as between the lumen and the plaque region in patients, based only on the optoacoustic detection of hemoglobin and lipid content. Specificity, sensitivity and accuracy of MSOT for imaging carotid atherosclerosis is expected to be explored in more extensive studies. In summary, MSOT: i) offers enriched complementary information to purely morphological US imaging and ii) opens new possibilities, not only for research on carotid atherosclerosis, but also for clinical decision making by exploring novel image-based biomarkers for the detection of the unstable plaque in future patients.

Declaration of Competing Interest

Prof. Dr. V. Ntziachristos is a stock owner of iThera Medical GmbH, Munich, Germany. All other authors declare no financial interests.

Acknowledgments

This project has received funding from the European Research Council (ERC) under the European Union's Horizon 2020 research and innovation program under grant agreement No 694968 (PREMSOT) and was supported by the DZHK (German Centre for Cardiovascular Research) and by the Helmholtz Zentrum München, funding program "Physician Scientists for Groundbreaking Projects".

References

[1] A. Saxena, E.Y.K. Ng, S.T. Lim, Imaging modalities to diagnose carotid artery stenosis: progress and prospect, Biomed. Eng. Online 18 (2019).
[2] R. Piri, O. Gerke, P.F. Høilund-Carlsen, Molecular imaging of carotid artery atherosclerosis with PET: a systematic review (in eng), Eur. J. Nucl. Med. Mol. Imaging (Nov) (2019).
[3] M. Naghavi, et al., From vulnerable plaque to vulnerable patient: a call for new definitions and risk assessment strategies: part I, Circulation 108 (2003) 1664–1672.
[4] M.M. Meloni, S. Barton, L. Xu, J.C. Kaski, W. Song, T. He, Contrast agents for cardiovascular magnetic resonance imaging: an overview (in eng), J. Mater. Chem. B 5 (August (29)) (2017) 5714–5725.
[5] W.A. Edelstein, M. Mahesh, J.A. Carrino, MRI: time is dose–and money and versatility (in eng), J. Am. Coll. Radiol. 7 (August (8)) (2010) 650–652.
[6] M. Mohammadshahi, M. Alipouri Sakha, A. Esfandiari, M. Shirvani, A. Akbari Sari, Cost effectiveness of mobile versus fixed computed tomography and magnetic resonance imaging: a systematic review (in eng), Iran. J. Public Health 48 (August (8)) (2019) 1418–1427.
[7] A. Karlas, et al., Flow-mediated dilatation test using optoacoustic imaging: a proof-of-concept, Biomed. Opt. Express 8 (7) (2017) 3395–3403, 2017/07/01.
[8] H. Yang, et al., Soft ultrasound priors in optoacoustic reconstruction: improving clinical vascular imaging (in eng), Photoacoustics 19 (September) (2020) 100172.
[9] A. Karlas, et al., Multispectral optoacoustic tomography of muscle perfusion and oxygenation under arterial and venous occlusion - a human pilot study, J. Biophotonics (March) (2020) p. e201960169, (in eng).
[10] A.P. Regensburger, et al., Detection of collagens by multispectral optoacoustic tomography as an imaging biomarker for Duchenne muscular dystrophy (in eng), Nat. Med. 25 (December (12)) (2019) 1905–1915.
[11] A. Karlas, et al., Multispectral optoacoustic tomography of peripheral arterial disease based on muscle hemoglobin gradients-a pilot clinical study (in eng), Ann. Transl. Med. 9 (January (1)) (2021) 36.
[12] J. Reber, et al., Non-invasive measurement of brown fat metabolism based on optoacoustic imaging of hemoglobin gradients, Cell Metab. 27 (3) (2018) 689–701, e4.
[13] A. Karlas, J. Reber, E. Liapis, K. Paul-Yuan, V. Ntziachristos, Multispectral optoacoustic tomography of brown adipose tissue (in eng), Handb. Exp. Pharmacol. 251 (2019) 325–336.
[14] N.-A. Fasoula, et al., Multicompartmental non-invasive sensing of postprandial lipemia in humans with multispectral optoacoustic tomography, Mol. Metab. (2021) 101184, 2021/02/05/.
[15] A. Karlas, M.A. Pleitez, J. Aguirre, V. Ntziachristos, Optoacoustic imaging in endocrinology and metabolism (in eng), Nat. Rev. Endocrinol. (April) (2021).
[16] A. Karlas, et al., Cardiovascular optoacoustics: from mice to men - a review (in eng), Photoacoustics 14 (June) (2019) 19–30.
[17] K.B. Chowdhury, J. Prakash, A. Karlas, D. Justel, V. Ntziachristos, A synthetic total impulse response characterization method for correction of hand-held optoacoustic images (in eng), IEEE Trans. Med. Imaging (April) (2020).
[18] D. Razansky, et al., Multispectral optoacoustic tomography of matrix metalloproteinase activity in vulnerable human carotid plaques, Mol. Imaging Biol. 14 (3) (2012) 277–285.
[19] M. Seeger, A. Karlas, D. Soliman, J. Pelisek, V. Ntziachristos, Multimodal optoacoustic and multiphoton microscopy of human carotid atheroma (in eng), Photoacoustics 4 (no. 3) (2016) 102–111.
[20] P. Song, et al., Global and regional prevalence, burden, and risk factors for carotid atherosclerosis: a systematic review, meta-analysis, and modelling study (in eng), Lancet Glob. Health 8 (May (5)) (2020) e721–e729.
[21] H.C. Stary, et al., A definition of advanced types of atherosclerotic lesions and a histological classification of atherosclerosis: a report from the committee on vascular lesions of the council on arteriosclerosis, American Heart Association, Circulation 92 (1995) 1355–1374.
[22] N.K. Chlis, et al., A sparse deep learning approach for automatic segmentation of human vasculature in multispectral optoacoustic tomography (in eng), Photoacoustics 20 (December) (2020) p. 100203.

Angelos Karlas studied Medicine (M.D.) and Electrical and Computer Engineering (Dipl.-Ing.) at the Aristotle University of Thessaloniki, Greece. He holds a Master of Science in Medical Informatics (M.Sc.) from the same university and a Master of Research (M.Res., DIC) in Medical Robotics and Image-Guided Interventions from Imperial College London, UK. He is currently working as clinical resident at the Department for Vascular and Endovascular Surgery at the Rechts der Isar University Hospital in Munich, Germany. He is also the Group Leader of the interdisciplinary Clinical Bioengineering Group at the Helmholtz Center Munich, Germany. He has already submitted his PhD thesis (Dr.rer.nat.) in Experimental Medicine at the Technical University of Munich, Germany. In the past, he served as the Clinical Translation Manager at the Institute for Biological and Medical Imaging of the Helmholtz Center Munich, Germany, as well as, the Junior Group Leader of the Clinical Translation Group at the same institute. His main research interests are in the areas of innovative vasometabolic imaging and image-guided vascular interventions.